Source Depletion Analogy for Reactive Plume Dispersion over Schematic Urban Areas

Zhangquan Wu and Chun-Ho Liu*

Department of Mechanical Engineering, The University of Hong Kong, Hong Kong

Revised Manuscript
Ms. Ref. No.: ATMENV-D-17-01702R1
submitted
to
Atmospheric Environment
as
Technical Note
on
June 19, 2018.

**Corresponding author address:*
Chun-Ho LIU
Department of Mechanical Engineering
7/F, Haking Wong Building
The University of Hong Kong
Pokfulam Road, Hong Kong, CHINA
Tel: (852) 3917 7901
Fax: (852) 2858 5415
E-mail: liuchunho@graduate.hku.hk

Source Depletion Analogy for Reactive Plume Dispersion over Schematic Urban Areas

Zhangquan Wu and Chun-Ho Liu

Department of Mechanical Engineering, The University of Hong Kong, Hong Kong

June 19, 2018

Abstract

Gaussian plume models have been used to estimate pollutant distribution for decades. In view of the empirically determined dispersion coefficients (largely based on atmospheric stability) , their application in urban setting needs to be interpreted cautiously. It is even more complicated if chemically reactive pollutants are considered. In this technical note, we examine the reactive plume dispersion over schematic urban areas in attempt to excel the functionality of the conventional Gaussian plume models. Open-channel flows over an array of identical ribs in crossflows serve the theoretical platforms of atmospheric surface layer (ASL) over buildings. The irreversible ozone O_3 titration oxidizes nitric oxide NO to nitrogen dioxide NO_2, representing the typical anthropogenic air pollution chemistry. Large-eddy simulation (LES) is employed to calculate the flows and pollution physics/chemistry coupling around/over the explicitly resolved roughness elements. The LES results show that, unlike the (larger) mesoscale ones, the conventional approach of modifying dispersion coefficients in terms of the timescales of pollution physics/chemistry is inapplicable due to inhomogeneous vertical mixing. We thus switch to the source depletion analogy which, however, estimates well the NO concentrations only above the plume rise mean height. A noticeable discrepancy is caused by the dominated NO oxidation in the near-wall region. Finally, the regression of LES output shows that the vertical dimensionless NO concentrations exhibit the Gamma γ-distribution for a range of background O_3 concentrations, unveiling a new, primitive parameterization of reactive plume dispersion over urban areas.

Keywords: Dispersion coefficient σ_z, Gaussian plume models, large-eddy simulation (LES), ozone O_3 titration, reactive nitric oxide NO plume transport and schematic urban areas.

1 Introduction

Air pollution poses major threat to premature mortality (Lelieveld et al. 2015) but its levels over 80% of the cities in the world are unhealthy (WHO 2016). Most air pollutants

are chemically reactive that evolve to their secondary counterparts in the atmospheric boundary layer (ABL). The conventional Gaussian plume model (Roberts 1923) has been widely employed in practical problems (Moreira et al. 2006), regulatory enactment (Briant et al. 2013), air toxic assessment (Scheffe et al. 2016) as well as continental pollutant transport (Tsuang et al. 2003). Its results, however, must be interpreted cautiously because of the inert-pollutant assumption (Harrison and McCartney 1980) and the complicated near-wall turbulent transport processes in the atmospheric surface layer (ASL; Britter and Hanna 2003).

In view of dense buildings, dispersion schemes have been developed to handle the rapid mixing in urban ASLs (Briggs 1973). The widening plume coverage is attributed to the elevated turbulence kinetic energy (TKE) in response to ground-level aerodynamic resistance (Walcek 2002). Early Gaussian plume models adopted the power-law wind profile (Sharma and Myrup 1975) together with the empirically determined dispersion coefficients (Skupniewicz and Schacher 1986) to handle the enhanced pollutant transport over urban areas. Whereas, the solution approach was basically site specific (Venkatram et al. 2005) that hindered from the understanding of fundamental mechanism. Extensive field measurements (Mavroidis and Griffiths 2001), laboratory experiments (Chung et al. 2015) and mathematical modeling (Inagaki et al. 2012) have been conducted to elucidate the influence of rough surfaces on ASL transport processes. However, the functional form of plume dispersion is not yet developed likely because of complicated urban morphology.

ABL pollutants are seldom mixed uniformly with ambient air in view of the inhomogenity in both flows and sources (Georgopoulos and Seinfeld 1986). Chemical kinetics and dynamics are therefore coupled with each other to modify the pollutant compositions which, however, are often ignored in reactive plume dispersion models (Chiogna et al. 2010). Mathematical modeling has been adopted for air pollution physics/chemistry coupling, such as the chemical evolution of nitrogen oxides NO_x (= NO + NO_2; where NO and NO_2 are nitric oxide and nitrogen dioxide, respectively), for decades (Lamb and Seinfeld 1973). In the engineering community, modeling turbulent transport by computational fluid dynamics (CFD) is generally grouped into stochastic (Bullin and Dukler 1974),

deterministic (Wang and Zhang 2009) and large-eddy simulation (LES; Tseng et al. 2006).

Simple, non-CFD models, such as AERMOD (USEPA 2016) and CALINE4 (Benson 1984), possess the benefit of quick solution together with the ability performing multiple simulations concurrently. To the authors' best knowledge, perhaps due to the challenging pollution physics/chemistry coupling in inhomogeneous flows, there is no non-CFD model developed so far for reactive plume dispersion over urban areas. It therefore motivates our interest in rapid, non-CFD modeling techniques for pollutant-concentration estimates. This section introduces the problem background and reviews the existing literature. The theory of reactive plume dispersion is detailed in Section 2. The solution approach, computation configuration and numerical methods are described in Section 3. The findings, especially the turbulent transport processes and the newly proposed non-CFD, reactive plume parameterization (Gamma γ-distribution), are reported in Section 4. Conclusions are finally drawn in Section 5.

2 Theoretical Background

The irreversible ozone O_3 titration

$$NO + O_3 \xrightarrow{k_3} NO_2 + O_2 \tag{1}$$

is considered where O_2 is oxygen molecule and k_3 ($= 0.411$ ppm^{-1} sec^{-1}) the chemical reaction rate constant at 293.15 K. The consumption (production) rates of nitric oxide and ozone (nitrogen dioxide) by chemistry Equation (1) are equal to

$$\frac{d\overline{c}_{NO}}{dt} = \frac{d\overline{c}_{O_3}}{dt} = -\frac{d\overline{c}_{NO_2}}{dt} = -k_3 \times \overline{c}_{NO} \times \overline{c}_{O_3} \tag{2}$$

where c_ϕ is the concentration of chemical species ϕ and overbar $\overline{\psi}$ the resolved-scale component in the LES. Hence, the chemistry timescales of nitric oxide $\tau_{NO} = 1/k_3\overline{c}_{O_3}$ and ozone $\tau_{O_3} = 1/k_3\overline{c}_{NO}$. Given the model configuration of uniform inflows doped with a constant background ozone concentration $[O_3]_0$, our preliminary LES results show that the ozone consumption $\Delta[O_3]$ ($= [O_3]_0 - \langle\overline{c}_{O_3}\rangle$ where angle brackets $\langle\psi\rangle$ denote the ensemble averaged properties) is less than 10%. We therefore essentially assume a constant chemistry timescale of nitric oxide $\tau_{NO} = 1/k_3[O_3]_0$ in the following analyses.

3 Methodology

3.1 Mathematical model

LES of the open-source CFD code Open-FOAM 2.3.0 (OpenFOAM 2015) is used in this technical note. The flows are assumed to be isothermal and incompressible that are calculated by the continuity and the Navier-Stokes equations in filtered variables. Source terms $\mathcal{S}_\phi$, which handle the chemical kinetics in the irreversible ozone titration Equation (1), are integrated into the filtered convection-diffusion equation

$$\frac{D}{Dt}\phi = \mathcal{D}(\phi) + \mathcal{S}_\phi \tag{3}$$

for the transport of chemical species ϕ where D/Dt is the material derivative and $\mathcal{D}(\phi)$ the diffusion term. Here, the source terms in the transport equations of NO, NO_2 and O_3 are $\mathcal{S}_{NO}$ $(= -k_3\overline{c}_{NO}\overline{c}_{O_3})$, $\mathcal{S}_{NO_2}$ $(= k_3\overline{c}_{NO}\overline{c}_{O_3})$ and $\mathcal{S}_{O_3}$ $(= -k_3\overline{c}_{NO}\overline{c}_{O_3})$, respectively. Hence, the source terms for NO and O_3 are consumptions while NO_2 production. The subgrid-scale (SGS) motions are modeled by the Smagorinsky model (Smagorinsky 1963). The one-equation SGS model is employed to enforce SGS TKE conservation (Schumann 1975). Only resolved scales are included in the source terms $\mathcal{S}_\phi$. The timescales are compared by the dimensionless Damköhler number Da $(= \tau_p/\tau_\phi$; where τ_p and τ_ϕ are the timescales of physical and chemical processes, respectively; Janssen et al. 1990). We focus on the mixing processes so the diffusion timescale τ_d is used to measure the physical processes. We look into the reactive plume dispersion of nitric oxide so its chemical timescale τ_{NO} is used to measure the chemical processes.

The LES model for schematic urban area consists of a number of idealized urban street canyons fabricated by identical square ribs of size h (Figure 1). The spatial domain sizes $72h$ (length) $\times$ $12h$ (width) $\times$ $12h$ (height) that is composed of 36 idealized street canyons of the same geometry. The street width b is the same as the building height h so the building-height-to-street-width (aspect) ratio is equal to unity. The flows thus fall into the skimming flow regime (Oke 1988). The prevailing flows in the urban ASL are driven by the (background) pressure gradient perpendicular to the street axes, representing the worst scenario of pollutant removal from street canyons. Ensemble average of the LES-calculated

pollutant concentrations $\langle \overline{c}_\phi \rangle$ is applied in the homogeneous spanwise y direction in the data analyses. The infinitely long streamwise x domain for flows is constructed by periodic boundary conditions (BCs). Wall BCs are applied on all the solid boundaries and shear-free BCs ($\partial\overline{u}/\partial z = \partial\overline{v}/\partial z = \overline{w} = 0$) along the domain top $z = H$. The prevailing wind enters the computational domain from the upstream inflow doped with a constant background ozone concentration $[\mathrm{O_3}]_0$. The sensitivity to NO chemistry timescales τ_{NO} is tested by controlling $[\mathrm{O_3}]_0$ (Table 1). An area source of nitric oxide with constant concentration $[\mathrm{NO}]_0$ is placed on the ground surface of the first street canyon that serves as a reactive pollutant being continuously emitted into the computational domain, simulating the vehicular exhaust in urban areas. Neumann BCs of pollutants ($\partial\overline{c}_\phi/\partial z = 0$) are applied on the remaining solid and shear-free boundaries. An open BC of pollutants ($\partial\overline{c}_\phi/\partial t + \overline{u}\ \partial\overline{c}_\phi/\partial x = 0$) is prescribed at the downstream outflow so all the chemical species are removed from the computational domain without reflection. The entire computational domain is discretized into 4.6×10^6 (hexahedral) cells approximately.

3.2 Modified Dispersion Coefficient

Analytical solution, following Sutton (1953) and Seinfeld (1986), to the advection-diffusion equation of a first-order chemically reactive pollutant at a consumption rate proportional to its local concentration $d\overline{c}_\phi/dt = -\mathcal{L}\overline{c}_\phi = -k_3 \times [\mathrm{O_3}]_0 \times \overline{c}_{\mathrm{NO}}$ in reactive nitric oxide plume exhibits the Gaussian form in which the modified pollutant dispersion coefficient is given by (Wu and Liu 2016*a*)

$$\widehat{\sigma}_z(x) = \frac{\sigma_z(x)}{(1 + 2\mathcal{K}\mathcal{L}/U^2)^{1/2}} = \frac{\sigma_z(x)}{[1 + 2(\tau_a/\tau_d \times \tau_a/\tau_{\mathrm{NO}})]^{1/2}} \tag{4}$$

where $\sigma_z(x)$ is the dispersion coefficient of inert pollutants in the streamwise direction x and $\mathcal{K}$ the (constant) eddy diffusivity. Uniform flows with a constant wind speed U is assumed so τ_a ($= h/U$; where h is the size of roughness elements) and τ_d ($= h^2/\mathcal{K}$) are the timescales of advection and diffusion, respectively. Equation (4) is in line with that has been reported in McKenna (1997) and Dore et al. (2015) in which the timescales of the dynamics and the chemistry are tightly coupled with each other, modifying the pollutant concentrations collectively. Hence, the classic assumption of diluent reactive gases with

negligible pollution physics/chemistry coupling (i.e. well-mixed conditions with prolonged τ_{NO}) should be applied cautiously in the ASL over urban areas. The discrepancy is more noticeable when the variation in the ratio of residence time scales, which is defined as the ratio of advection-time-scale-to-diffusion-time-scale τ_a/τ_d, is large in the vertical direction. The modified dispersion coefficient $\widehat{\sigma}_z$ is no longer a function of streamwise distance x only that violates the prime assumption of Gaussian plume models (dispersion coefficient is a function of streamwise distance x after the source that is independent from the vertical height z; Wu and Liu 2016*b*) . This finding arouses our interest to improve the current parameterization of reactive plume dispersion in the inhomogeneous ASL over urban areas.

3.3 Source Depletion Analogy

In view of the variation in physical timescales τ_a and τ_d across the urban ASL, the conventional approach of modified pollutant dispersion coefficient Equation (4) is no longer applicable to reactive plume. Because the chemistry is dominated in the near-wall region, we modify the Gaussian plume model by source depletion analogy (Arya 1998) in attempt to handle ozone titration Equation (1) by a non-CFD model. As a preliminary study, the depleted source is calculated by integrating the mean streamwise pollutant flux across the turbulent boundary layer

$$Q_{dp}(x) = \int_0^H \langle \overline{u}(x,z) \rangle \times \langle \overline{c}_{\mathrm{NO}}(x,z) \rangle \; dz \; . \tag{5}$$

4 Results and Discussion

4.1 Flow and Turbulence Structure

Figure 2 depicts the flow and turbulence properties in the urban ASL over the rib-type schematic urban surface described previously. The mean-wind speed profile (Figure 2a) agrees well with our previous wind tunnel measurement (Ho and Liu 2017) but over-predicts slightly than that available in literature (Wood and Antonia 1975). The mild dissimilarity is attributed to the different roughness Reynolds number Re_* ($= u_* h/\nu$; where u_* is the friction velocity and ν the kinematic viscosity) that was approximately 60

in Wood and Antonia (1975), was over 600 in Ho and Liu (2017) and is 470 in this paper.

The sharp near-wall wind-speed gradient signifies the locally elevated TKE also. The streamwise $\langle u''u''\rangle^{1/2}$ (Figure 2b) and the vertical $\langle w''w''\rangle^{1/2}$ (Figure 2c) fluctuating velocities are normalized by the friction velocity u_* instead of the prevailing wind speed u_∞ similar to most studies of turbulent shear flows. Here, the angle bracket $\langle\psi\rangle$ denotes spatio-temporally (ensemble) averaged properties (horizontal domain for flows and spanwise domain for pollutants) and the double prime denotes the deviation of the property from its ensemble average $\psi'' = \overline{\psi} - \langle\overline{\psi}\rangle$. A good agreement of fluctuating velocities, especially in the lower urban ASL, between the current LES and the wind tunnel measurements (Burattini et al. 2008, Ho and Liu 2017) is observed. Minor differences, such as a higher LES-calculated streamwise fluctuating velocity $\langle u''u''\rangle^{1/2}$ compared with that of the direct numerical simulation (DNS) of Coceal et al. (2007), are found. The current LES-calculated streamwise fluctuating velocity (Figure 2b) agrees well with that of the wind tunnel measurements of Krogstad and Antonia (1999) but underpredicts the vertical component (Figure 2c). Besides, the LES-calculated fluctuating velocities in both streamwise and vertical direction are smaller than the wind tunnel measurements of Djenidi et al. (1999). Apart from the different Reynolds number, the aforementioned discrepancy in various aspects is likely attributed to the dissimilar turbulence generation mechanism in mathematical models and laboratory experiments. Horizontally homogeneous flows are assumed in the current LES so the turbulence is generated only by the interaction between momentum flux $\langle u''w''\rangle$ and gradient of mean-wind speed $\partial\langle\overline{u}\rangle/\partial z$, resulting in a TKE intensity smaller than that of laboratory measurements.

As shown in Figure 2d, both our previous wind-tunnel measurements (Ho and Liu 2017) and the current LES results exhibit the conventional characteristics of ensemble averaged vertical momentum flux $\langle u''w''\rangle$ in turbulent shear flows that decreases with increasing height. The wind-tunnel measurements deviate slightly from linearity because of the background turbulence intensity ($\approx 10\%$). On the other hand, the LES-calculated total momentum flux ($= \langle u''w''\rangle - \tau_{xz} - \nu\partial\langle\overline{u}\rangle/\partial z$; where τ_{xz} is the SGS momentum flux) is almost linearly proportional to the wall-normal distance z that agrees well with the

theoretical solution. The small SGS and viscous momentum fluxes support that the LES spatial resolution is sufficient. Whereas, the layer of constant momentum flux in the near-wall region is shallow compared with that of the wind tunnel measurements.

4.2 Inert Plume Dispersion

Nitrogen conserves in the sensitivity tests regardless of the background ozone concentrations $[O_3]_0$ so the nitrogen oxides NO_x plume can be taken as inert-pollutant dispersion. Figure 3a depicts the dimensionless profiles of nitrogen oxides concentration $\langle \overline{c}_{NO_x} \rangle$ as functions of wall-normal distance z at different streamwise locations x. The current LES-calculated concentrations agree well with the theoretical Gaussian-form solutions. Scaled concentration profiles of nitrogen oxides are independent from the streamwise location x in which the dispersion coefficient is calculated by

$$\sigma_z(x) = \left[\frac{\int_{z=0}^{z=H} \langle \overline{c}_{NO_x}(x,z) \rangle \, z^2 \, dz}{\int_{z=0}^{z=H} \langle \overline{c}_{NO_x}(x,z) \rangle \, dz} \right]^{1/2} . \tag{6}$$

In view of the rapid change of LES-calculated mean-wind speed $\langle \overline{u} \rangle$ in the near-wall region, the average mean-wind speed across 95% of plume coverage

$$\widehat{u} = \frac{\int_{z=0}^{z=2\sigma_z} \langle \overline{u}(z) \rangle \, dz}{\int_{z=0}^{z=2\sigma_z} dz} \tag{7}$$

is introduced in the analysis to facilitate the comparison between the LES and analytical solutions.

The far-field behavior $\sigma_z \propto x^{1/2}$ might not be fully developed in the near-field plume dispersion so a noticeable discrepancy between the theoretical Gaussian plume model and the current LES is observed at $x = 15.5h$. In the near-wall region $z \leq 0.25 \times 2^{1/2}\sigma_z$ right over the roughness elements, the current LES shows a higher level of inert-pollutant concentrations than does the analytical Gaussian solution by 10%. In addition to the elevated near-wall wind-speed gradient, the difference could be attributed to the pollutant reflection from the ground surface, which, however, cannot be simply represented by the

method of reflection and superposition for plume dispersion. Moreover, the slower flows suppress the pollutant dilution over rough surfaces.

4.3 Reactive Plume Dispersion

Including chemistry in the LES results in an obvious plume rise mean height

$$z_r\left(x\right)=\frac{\int_{z=0}^{z=H}\left\langle \overline{c}_{\mathrm{NO}}\left(x,z\right)\right\rangle z\ dz}{\int_{z=0}^{z=H}\left\langle \overline{c}_{\mathrm{NO}}\left(x,z\right)\right\rangle \ dz} \tag{8}$$

in terms of the streamwise location x. The consumption of nitric oxide by ozone titration is much more significant in the near-wall region so the peaked concentrations of nitric oxides are elevated (Figure 3). The plume rise mean height z_r increases with increasing background ozone concentration $[\mathrm{O_3}]_0$ that varies over five times from $z_r = 0.1 \times 2^{1/2}\sigma_z$ for $[\mathrm{O_3}]_0 = 1$ ppb up to $z_r = 0.6 \times 2^{1/2}\sigma_z$ for $[\mathrm{O_3}]_0 = 500$ ppb. The deviation from Gaussian solution can be explained by the change in Damköhler number so the relative extent of physical/chemical processes is nonuniform in the wall-normal direction. Hence, applying the conventional Gaussian plume model to reactive plume dispersion must be careful because the fully well-mixed conditions are seldom complied with. In particular, the primary-pollutant concentrations would be under-predicted because of secondary-pollutant production.

Figure 3 compares the dimensionless profiles of nitric oxide concentrations $\langle \overline{c}_{\mathrm{NO}} \rangle$ in different background ozone concentrations $[\mathrm{O_3}]_0$. The source of nitric oxide in the theoretical Gaussian plume model is depleted in order to handle the ozone titration (Equation 5). The LES-calculated dimensionless nitric oxide concentration at different streamwise locations clearly exhibit self-similarity, supporting the validity of Gaussian-shape functional form of the source depletion models for reactive plume dispersion. Alike their inert-pollutant counterpart, early plume-dispersion characteristics are clearly observed in the near field at $x = 15.5h$ where the plume dispersion is not yet fully developed, deviating from the self-similarity. It is caused by the implicit limitation of Gaussian plume model. Ozone titration is nonuniform that is dominated in the near-wall region where a sharp drop in local nitric concentrations is observed, unveiling the drawback of Gaussian solution

to reactive plume dispersion. The nitric oxide concentrations decrease with increasing background ozone concentrations. Almost all the nitric oxide in the near-wall region is consumed in the case of high-level background ozone concentration $[O_3]_0 = 500$ ppb so the functional form of concentration distribution does not fully follow Gaussian shape. This is another major limitation of the source depletion model, calling for an alternative solution to reactive plume dispersion.

For the far-field nitric oxide concentrations $\langle \overline{c}_{NO} \rangle$, the analytical Gaussian-form source depletion plume model and the current LES-calculated results exhibit various degrees of disagreement in response to the background ozone concentrations $[O_3]_0$, i.e. different chemistry timescales τ_{NO}. An obvious discrepancy in nitric oxide concentrations , which increases with increasing background ozone concentration, is observed in the near-wall region. Ozone governs the life time of nitric oxide in the plume dispersion. Higher background ozone concentrations shorten the life time of nitric oxide τ_{NO}. The effect is more promising for a longer residence time such as in the near-wall region where turbulent diffusion dominates the transport processes, i.e. residence is determined by the diffusion timescale τ_d. The discrepancy diminishes with increasing wall-normal distance because of the reducing residence time in advection-dominated transport processes. It is interesting that the error is noticeable mainly below the plume rise mean height z_r. Over the plume rise mean height the prediction of the newly developed source depletion analogy is good, suggesting a handy parameterization of reactive plume dispersion.

4.4 Reactive Plume Parameterization

In view of the discrepancy in the calculation of nitric oxide concentrations $\langle \overline{c}_{NO} \rangle$ observed below the plume rise mean height, additional effort is sought to improve the reactive plume dispersion parameterization. We focus on the near-wall region below the plume rise mean height $z \leq z_r$ where the source depletion analogy shows a major over-prediction in ground-level nitric oxide concentration $\langle \overline{c}_{NO} \rangle$. Gamma γ-distribution in terms of γ function $\Gamma(\alpha)$

$$\sqrt{\frac{\pi}{2}} \times \frac{\widehat{u}\sigma_z}{Q_{dp}} \times \langle \overline{c}_{NO} \rangle = \frac{\left(z/\sqrt{2}\sigma_z\right)^{\alpha-1}}{\beta^{\alpha}\Gamma(\alpha)} \exp\left(-\frac{z/\sqrt{2}\sigma_z}{\beta}\right) \tag{9}$$

is tested by regression where α and β are parameters which can be determined by the mean μ ($= \alpha\beta$) and the variance σ^2 ($= \alpha\beta^2$) of the pollutant distribution. The reduction in nitric oxide concentrations below the plume rise mean height z_r in the near-wall region is predicted well by the Gamma γ-distribution (Figure 3). Over the plume rise mean height, both the Gaussian-form source depletion model and the Gamma γ-distribution show similar dimensionless profiles which are close to the current LES-calculated nitric oxide concentration. The root-mean-square (RMS) error between the nitric oxide concentrations $\langle \overline{c}_{\mathrm{NO}} \rangle$ in various background ozone concentrations $[\mathrm{O_3}]_0$ calculated by the source depletion model and the Gamma γ-distribution is tabulated in Table 1 as well. Except the one with $[\mathrm{O_3}]_0 = 10$ ppb, the Gamma γ-distribution outperforms the source depletion analogy in which the accuracy is improved substantially such that the RMS error is reduced by an order of magnitude. The improvement is more prominent at higher background ozone concentrations because the Gamma γ-distribution is able to handle well the rapid near-wall ozone titration.

Coincidentally, the Gamma γ-distribution was used to handle reactive plume dispersion over smooth surfaces in stochastic approaches (Ferrero et al. 2013). The large-scale plume meandering was calculated by stochastic equations and the internal mixing was modeled using bivariate Gamma function. No roughness element was considered. On the other hand, the Gamma γ-distribution was used to model the concentration probability density function (PDF) of plume dispersion over a large array of obstacles (Gailis et al. 2007). Although chemistry was not considered, the favorable agreement of using Gamma γ-distribution could be attributed to the strong mixing and rapid dilution of pollutants in the near-wall region. In this study, the LES results show that the plume shape is modified by ozone titration instead of surface roughness.

5 Conclusions

Gaussian plume model is well received in industry for the quick estimate of pollutant distribution in open-terrain configurations. Whereas, its functionality for reactive plume dispersion over urban areas is rather limited because most of the dispersion coefficients

were determined empirically as functions of atmospheric stability only yet overlooked surface roughness. The drawback on dynamics is thus often biased toward temperature stratification. The interaction between pollution physics and chemistry is more complicated because of the coupling between transport (τ_a and τ_d) and reaction (τ_ϕ) timescales. Hence, the conventional Gaussian plume model must be applied with caution to urban setting. In this technical note, we report a preliminary study of reactive plume dispersion over schematic urban areas in the form of identical ribs in crossflows (idealized urban street canyons). The LES flow properties over rough surfaces are similar to those of open-channel flows that agree well with other results available in literature. The irreversible ozone titration is adopted to demonstrate the effect of pollution chemistry on plume dispersion. Because ozone titration mainly takes place in the near-wall region but not evenly throughout the urban ASL, the LES results show that most nitric oxide is oxidized to nitrogen dioxide in the near-wall region so the dimensionless profiles of reactive plume dispersion is no longer Gaussian form. As such, we first use the analogous pollutant source depletion to handle the near-wall chemistry dominance. The source depletion analogy calculates well the reactive plume dispersion in the region over plume rise mean height z_r. However, the large difference in timescales in urban ASL, especially below the plume rise mean height, cannot be rectified. In view of the major discrepancy below the plume rise mean height, the Gamma γ-distribution is proposed as the regression to the pollutant distribution in which an appreciable improvement is clearly demonstrated. The current solution framework could in turn formulate a new, primitive parameterization of reactive plume dispersion over urban areas. Additional effort is undertaken to advance our understanding of the physics/chemistry mechanism as well as to refine the parameterization.

Acknowledgments

The first author wishes to thank the Hong Kong Research Grants Council (RGC) for financially supporting his study through the Hong Kong PhD fellowship (HKPF) scheme. This research is conducted in part using the research computing facilities and/or

advisory services offered by Information Technology Services (ITS), The University of Hong Kong (HKU). Technical support from Ms. Lilian Y.L. Chan, Mr. W.K. Kwan and Mr. Bill H.T. Yau is appreciated. This project is partly supported by the General Research Fund (GRF) of RGC HKU 17210115. Last but not least, we thank the anonymous reviewer for providing helpful critiques of the original manuscript.

References

Arya, S. P. S. (1998), *Air Pollution Meteorology and Dispersion*, Oxford University Press, Oxford.

Benson, P. E. (1984), *CALINE4 - A Dispersion Model for Predicting Air Pollutant Concentrations near Roadways*, Office of Transportation Laboratory, California Department of Transportation, Sacramento, California 95819.

Briant, R., Seigneur, C., Gadrat, M. and Bugajny, C. (2013), 'Evaluation of roadway gaussian plume models with large-scale measurement campaigns', *Geosci. Model Dev.* **6**, 445–456.

Briggs, G. A. (1973), 'Diffusion estimation for small emissions'. *Atmospheric Turbulence and Diffusion Laboratory contribution*, File No. 79.

Britter, R. E. and Hanna, S. R. (2003), 'Flow and dispersion in urban areas', *Annu. Rev. Fluid Mech.* **35**, 469–496.

Bullin, J. A. and Dukler, A. E. (1974), 'Stochastic modeling of turbulent diffusion with hybrid computer', *Environ. Sci. Technol.* **8**, 156–165.

Burattini, P., Leonardi, S., Orlandi, P. and Antonia, R. A. (2008), 'Comparison between experiment and direct numerical simulations in a channel flow with roughness on one wall', *J. Fluid Mech.* **600**, 403–426.

Chiogna, G., Eberhardt, C., Grathwohl, P., Cirpka, O. A. and Rolle, M. (2010), 'Evidence of compound-dependent hydrodynamic and mechanical transverse dispersion by multitracer laboratory experiments', *Environ. Sci. Technol.* **44**, 688–693.

Chung, J., Hagishima, A., Ikegaya, N. and Tanimoto, J. (2015), 'Wind-tunnel study of scalar transfer phenomena for surfaces of block arrays and smooth walls with dry patches', *Boundary-Layer Meteorol.* **157**, 219–236.

Coceal, O., Thomas, T. G. and Belcher, S. E. (2007), 'Spatial variability of flow statistics within regular building arrays urban-like cubical obstacles', *Boundary-Layer Meteorol.* **125**, 537–552.

Djenidi, L., Elavarasan, R. and Antonia, R. A. (1999), 'The turbulent boundary layer over transverse square cavities', *J. Fluid Mech.* **395**, 271–294.

Dore, A. J., Carslaw, D. C., Braban, C., Cain, M., Chemel, C., Conolly, C., Derwent, R. G., Griffiths, S. J., Hall, J., Hayman, G., Lawrence, S., Metacalfe, S. E., Redington, A., Simpson, D., Sutton, M. A., Sutton, P., Tang, Y. S., Vieno, M., Werner, M. and Whyatt, J. D. (2015), 'Evaluation of the performance of different atmospheric chemical transport models and inter-comparison of nitrogen and sulphur deposition estimates of the UK', *Atmo. Environ.* **119**, 131–143.

Ferrero, E., Mortarini, L., Alessandrini, S. and Lacagnina, C. (2013), 'Application of a bivariate gamma distribution for a chemically reacting plume in the atmosphere', *Boundary-Layer Meteorol.* **147**, 123–137.

Gailis, R. M., Hill, A., Yee, E. and Hilderman, T. (2007), 'Extension of a fluctuating plume model of tracer dispersion to a sheared boundary layer and to a large array of obstacles', *Boundary-Layer Meteorol.* **122**, 577–607.

Georgopoulos, P. G. and Seinfeld, J. H. (1986), 'Mathematical modeling of turbulent reacting plumes - I. general theory and model formulation', *Atmos. Environ.* **20**, 1791–1807.

Harrison, R. M. and McCartney, H. A. (1980), 'A comparison of the predictions of a simple gaussian plume dispersion model with measurements of pollutant concentration at ground-level and aloft', *Atmos, Environ.* **14**, 589–596.

Ho, Y.-K. and Liu, C.-H. (2017), 'A wind tunnel study of flows over idealised urban surfaces with roughness sublayer corrections', *Theor. Appl. Climatol.* **130**, 305–320.

Inagaki, A., Castillo, M. C. L., Yamashita, Y., Kanda, M. and Takimoto, H. (2012), 'Large-eddy simulation of coherent flow structures within a cubical canopy', *Boundary-Layer Meteorol.* **142**, 207–222.

Janssen, L. H. J. M., Nieuwstadt, F. T. M. and Donze, M. (1990), 'Time scales of physical and chemical processes in chemically reactive plumes', *Atmos. Environ.* **24A**, 2861–2874.

Krogstad, P.-A. and Antonia, R. A. (1999), 'Surface roughness effects in turbulent boundary layers', *Exp. Fluids* **27**, 450–460.

Lamb, R. G. and Seinfeld, J. H. (1973), 'Mathematical modeling of urban air pollution: General theory', *Environ. Sci. Technol.* **7**, 253–261.

Lelieveld, J., Evans, J. S., Fnais, M., Giannadaki, D. and Pozzer, A. (2015), 'The contribution of outdoor air pollution sources to premature mortality on a global scale', *Nature* **525**, 367–371.

Mavroidis, I. and Griffiths, R. F. (2001), 'Local characteristics of atmospheric dispersion within building arrays', *Atmos. Environ.* **35**, 2941–2954.

McKenna, D. S. (1997), 'Analytic solutions of reactive diffusion equations and implications for the concept of an air parcel', *J. Geophys. Res.* **102**, 13719–13725.

Moreira, D. M., Vilhena, M. T., Tirabassi, T., Costa, C. and Bodmann, B. (2006), 'Simulation of pollutant dispersion in the atmosphere by the Laplace transform: the ADMM approach', *Water, Air, and Soil Pollution* **177**, 411–439.

Oke, T. R. (1988), 'Street design and urban canopy layer climate', *Energy and Buildings.* **11**, 103–113.

OpenFOAM (2015), 'Openfoam: The open source CFD toolbox'. http://www.openfoam.com/.

Roberts, O. F. T. (1923), 'The theoretical scattering of smoke in a turbulent atmosphere', *Proc. Roy. Soc. London A* **104**, 640–654.

Scheffe, R. D., Strum, M., Phillips, S. B., Thurman, J., Eyth, A., Fudge, S., Morris, M., Palma, T. and Cook, R. (2016), 'Hybrid modeling approach to estimate exposures of hazardous air pollutants (HAPs) for the national air toxics assessment (NATA)', *Environ. Sci. Technol.* **50**, 12356–12364.

Schumann, U. (1975), 'Subgrid scale model for finite difference simulations of turbulent flows in plane channels and annuli', *J. Comp. Phys.* **18**, 376–404.

Seinfeld, J. H. (1986), *Atmospheric Chemistry and Physics of Air Pollution*, Johm Wiley & Sons, Inc., New York, USA.

Sharma, V. and Myrup, O. L. (1975), 'Diffusion from a line source in an urban atmosphere', *Atmos. Environ.* **9**, 907–922.

Skupniewicz, C. E. and Schacher, G. E. (1986), 'Parameterization of plume dispersion over water', *Atmos. Environ.* **20**, 1333–1340.

Smagorinsky, J. (1963), 'General circulation experiments with the primative equations I: The basic experiment', *Month. Weath. Rev.* **91**, 99–165.

Sutton, O. G. (1953), *Micrometeorology: A Study of Physical Processes in the Lowest Layer of the Earth's Atmosphere*, McGraw-Hill Book Company, Inc., New York, USA.

Tseng, Y.-H., Meneveau, C. and Parlange, M. B. (2006), 'Modeling flow around bluff bodies and predicting urban dispersion using large eddy simulation', *Environ. Sci. Technol.* **40**, 2653–2662.

Tsuang, B.-J., Lee, C.-T., Cheng, M.-T., Lin, N.-H., Lin, Y.-C., Chen, C.-L., Peng, C.-M. and Kuo, P.-H. (2003), 'Quantification on the source/receptor relationship of primary pollutants and seconsary aerosols by a Gaussian plume trajectory model: Part III - Asian dust-storm period', *Atmos. Environ.* **37**, 4007–4017.

402 USEPA (2016), *User's Guide for the AMS/EPA Regulatory Model (AERMOD)*, U.S. En-
403 vironmental Protection Agency, Research Triangle Park, North Carolina.

404 Venkatram, A., Isakov, V., Pankratz, D. and Yuan, J. (2005), 'Relating plume spread to
405 meteorology in urban areas', *Atmos. Environ.* **39**, 371–380.

406 Walcek, C. J. (2002), 'Effect of wind shear on pollution dispersion', *Atmos. Environ.*
407 **36**, 511–517.

408 Wang, Y. J. and Zhang, K. M. (2009), 'Modeling near-road air quality using a computa-
409 tional fluid dyanmics model, CFD-VIT-RIT', *Environ. Sci. Technol.* **43**, 7778–7783.

410 WHO (2016), 'WHO's urban ambient air pollution database - update 2016'. Public
411 Health, Social and Environmental Determinants of Health Department, World Health
412 Organization, 1211 Geneva 27, Switzerland; www.who.int/phe.

413 Wood, D. H. and Antonia, R. A. (1975), 'Measurements in a turbulent boundary layer
414 over a *d*-type surface roughness', *J. Appl. Mech.* **42**, 591–597.

415 Wu, Z. and Liu, C.-H. (2016*a*), Reactive plume dispersion over idealized urban roughness,
416 *in* '8$^{\text{th}}$ International Colloquium on Buff Body Aerodynamics and Applications'. June
417 7 to 11, 2016; Boston, Massachusetts, USA.

418 Wu, Z. and Liu, C.-H. (2016*b*), Study of chemically reactive pollutant transport over urban
419 roughness in the atmospheric boundary layer, *in* 'The 12th UK Wind Engineering
420 Society Conference (WES2016)'. September 5 to 7, 2016; Nottingham, UK.

Table 1: Root mean square (RMS) error comparing source depletion model and Gamma γ-distribution.

Background ozone	RMS error	
concentration $[O_3]_0$ (ppb)	Source depletion model	Gamma γ-distribution
1	0.009745	0.001761
10	0.0006537	0.002166
50	0.008048	0.002672
100	0.01582	0.002972
200	0.02984	0.003605
500	0.05867	0.004318

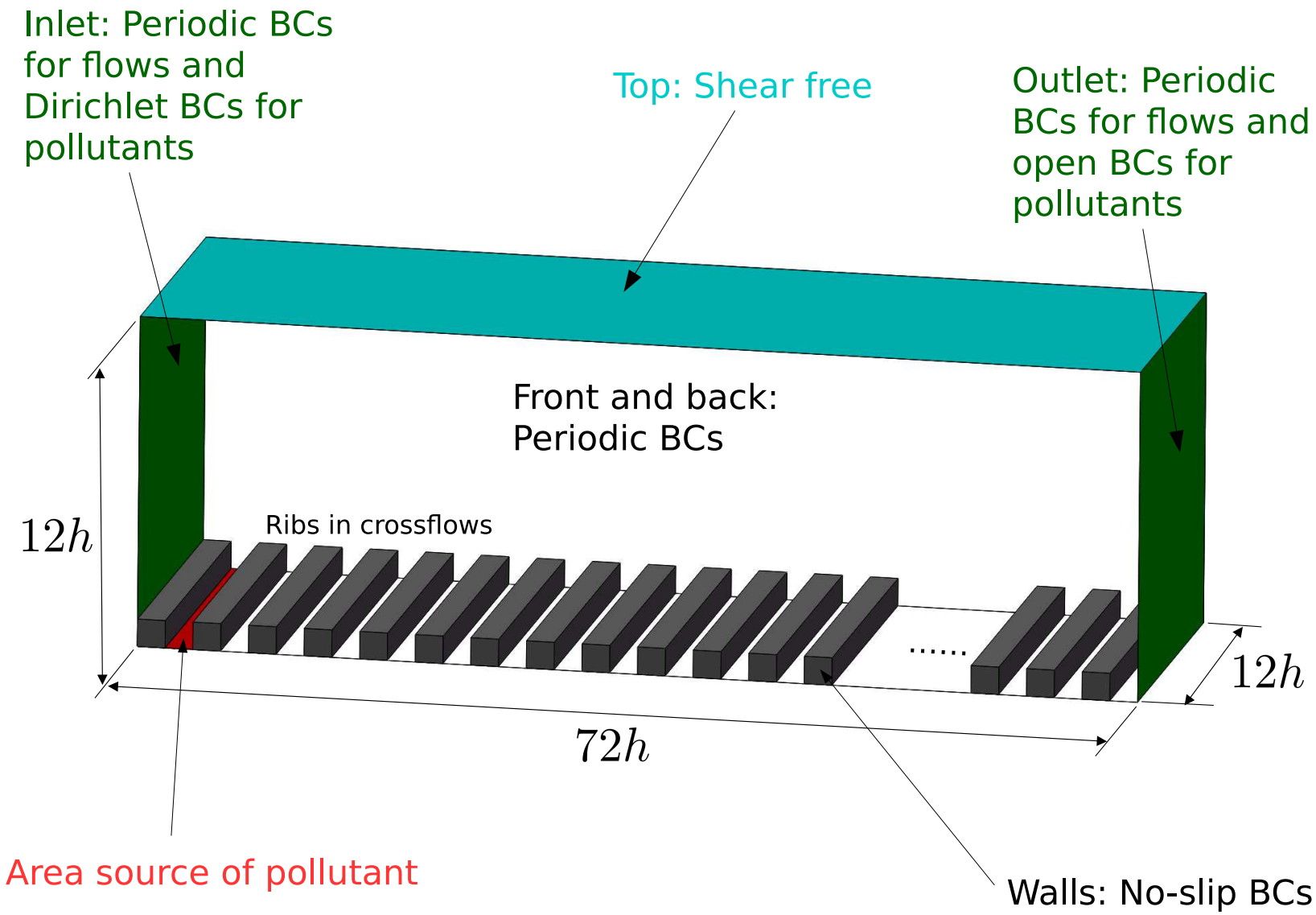

Figure 1: Spatial domain of the LES.

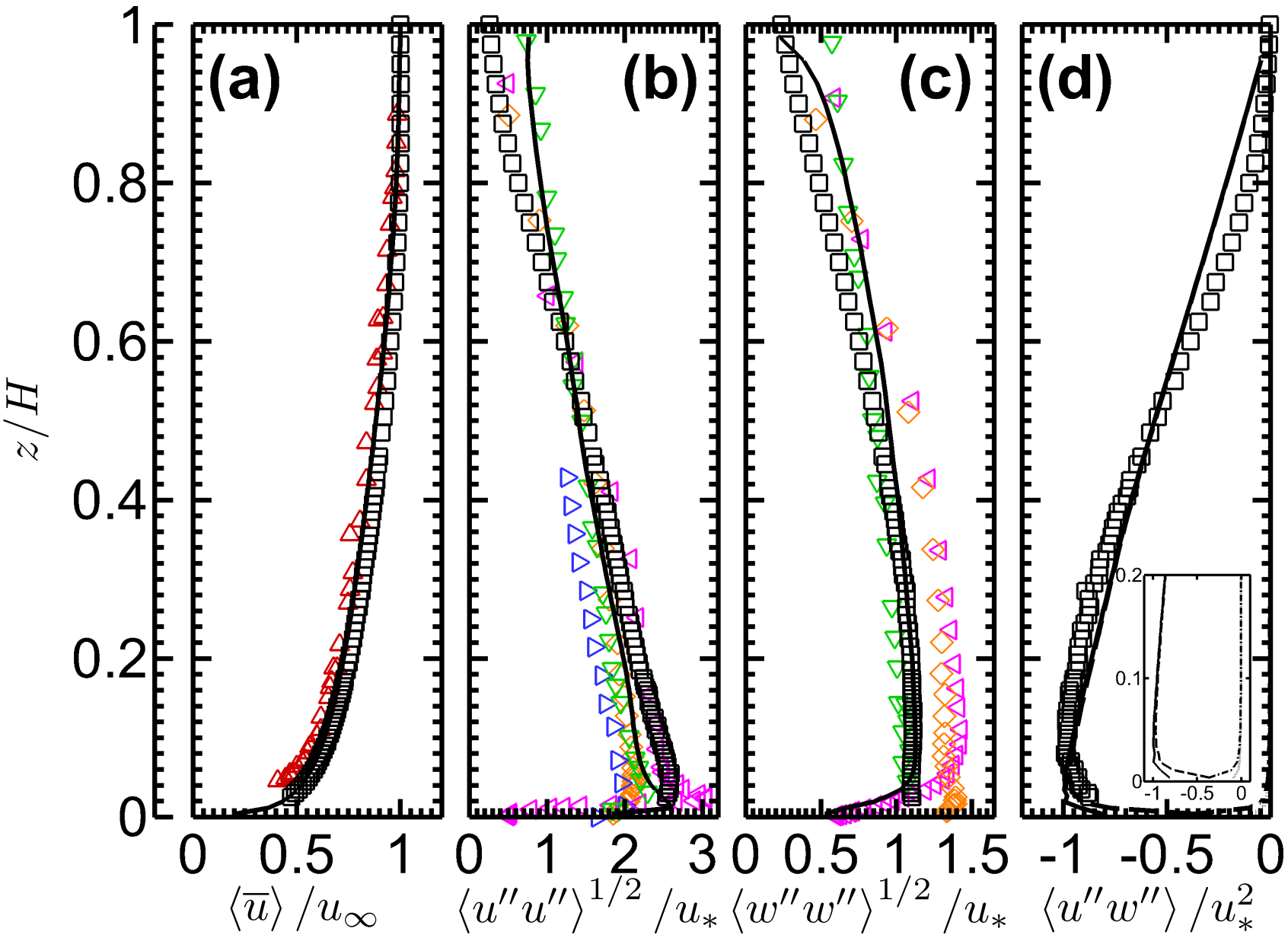

Figure 2: Dimensionless profiles of (a) mean wind speed $\langle \overline{u} \rangle / u_\infty$; (b) fluctuating streamwise velocity $\langle u''u'' \rangle^{1/2} / u_*$; (c) fluctuating vertical velocity $\langle w''w'' \rangle^{1/2} / u_*$ and (d) momentum flux $\langle u''w'' \rangle / u_*^2$ calculated by the current LES: —— expressed in dimensionless wall-normal coordinate z/H. Also shown are the measurement results of Wood and Antonia (1975): Δ; Djenidi et al. (1999): $\triangleleft$; Krogstad and Antonia (1999): $\diamond$; Burattini et al. (2008): ∇ and Ho and Liu (2017): $\square$ together with the DNS results of Coceal et al. (2007): $\triangleright$. The total momentum flux calculated by the current LES (——) is decomposed into the resolved scale (– – – – – –), the subgrid scale (– · – · – · – · – ·) and the viscous scale (· · · · · ·). The subgrid-scale and viscous-scale momentum fluxes are small compared with the resolved one so are shown in the inserted figure also.

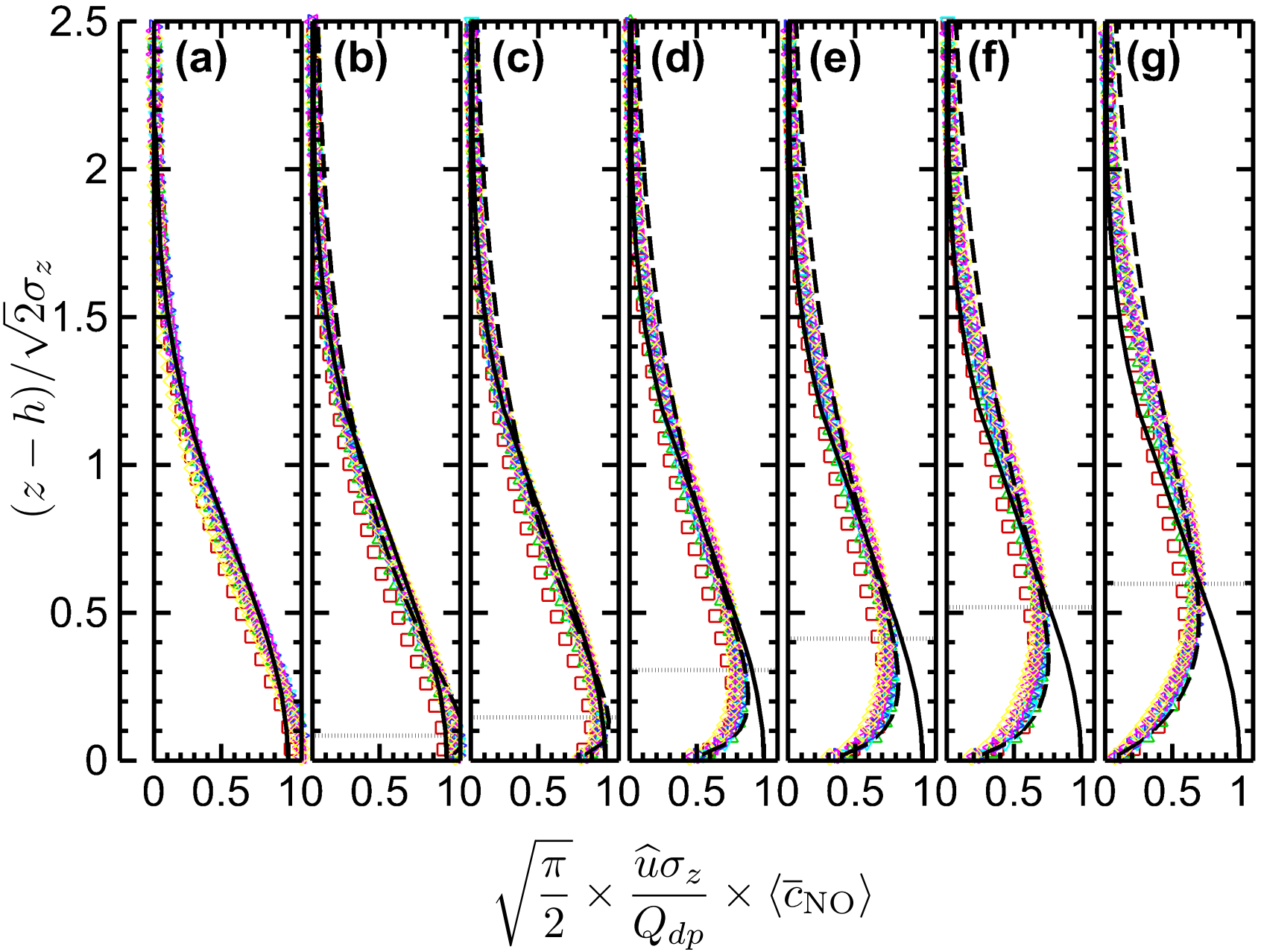

Figure 3: Dimensionless profiles of reactive pollutant nitric oxide concentration $(\pi/2)^{1/2} \times \widehat{u}\sigma_z/Q_{dp} \times \langle \overline{c}_{\mathrm{NO}} \rangle$ in the streamwise direction at $x/h =$ 15.5: □, 25.5: △, 35.5: ▽, 45.5: ▷, 55.5: ◁ and 65.5: ◇ expressed in dimensionless wall-normal coordinate $z/2^{1/2}\sigma_z$ for background ozone concentration $[\mathrm{O_3}]_0$ of (a) 0 ppb (insert pollutant nitrogen oxides $\mathrm{NO_x}$); (b) 1 ppb; (c) 10 ppb; (d) 50 ppb; (e) 100 ppb; (f) 200 ppb and (f) 500 ppb. Also shown are the profiles of the theoretical Gaussian plume model: —— and the Gamma γ-distribution: – – – – – – Equation (9). The plume-rise level z_r is indicated by ·····.